

Correction: Betulinic acid impairs metastasis and reduces immunosuppressive cells in breast cancer models

An-Qi Zeng^{1,*}, Yan Yu^{1,*}, Yu-Qin Yao^{1,*}, Fang-Fang Yang¹, Mengya Liao², Lin-Jiang Song¹, Ya-Li Li¹, Yang Yu³, Yu-Jue Li¹, Yuan-Le Deng¹, Shu-Ping Yang¹, Chen-Juan Zeng^{1,4}, Ping Liu⁵, Yong-Mei Xie¹, Jin-Liang Yang¹, Yi-Wen Zhang¹, Ting-Hong Ye¹ and Yu-Quan Wei¹

¹Laboratory of Liver Surgery, State Key Laboratory of Biotherapy, West China Hospital, Sichuan University and Collaborative Innovation Center for Biotherapy, Chengdu 610041, China

²Sichuan Nursing Vocational College, Chengdu 610100, China

³Department of Peritoneal Cancer Surgery, Beijing Shijitan Hospital Affiliated to the Capital Medical University, Beijing 100038, China

⁴Sichuan Scientist Biotechnology Co., Ltd, Chengdu 610041, China

⁵Department of Gynecology and Obstetrics, Key Laboratory of Birth Defects and Related Diseases of Women and Children of the Ministry of Education, West China Second Hospital, Sichuan University, Chengdu 610041, China

*These authors contributed equally to this work

Published: November 23, 2021

Copyright: © 2021 Zeng et al. This is an open access article distributed under the terms of the [Creative Commons Attribution License](https://creativecommons.org/licenses/by/3.0/) (CC BY 3.0), which permits unrestricted use, distribution, and reproduction in any medium, provided the original author and source are credited.

This article has been corrected: Due to errors in figure preparation, there are several instances of accidental overlapping images. In Figure 2B, the 'Control' and '20 μ M' images contain partial overlaps. In Figure 3E, the 'MMP-2 Vehicle' and 'MMP-2 BA' images contain partial overlaps. In Figure 1B, the first and second images in the '4T1' row contain partial overlaps. The third and fourth images in the 'MDA-MB-231' row contain partial overlaps. The final image in the '4T1' row and the fifth image in the 'MDA-MB-231' row contain partial overlaps. In addition, the first, second and third images in the 'MCF-7' row also contain partial overlaps. Finally, in Figure 5B, the second image in the 'BA' row is incorrect. The corrected Figures 1, 2, 3 and 5 are shown below. The authors declare that these corrections do not change the results or conclusions of this paper.

Original article: Oncotarget. 2018; 9:3794–3804. <https://doi.org/10.18632/oncotarget.23376>

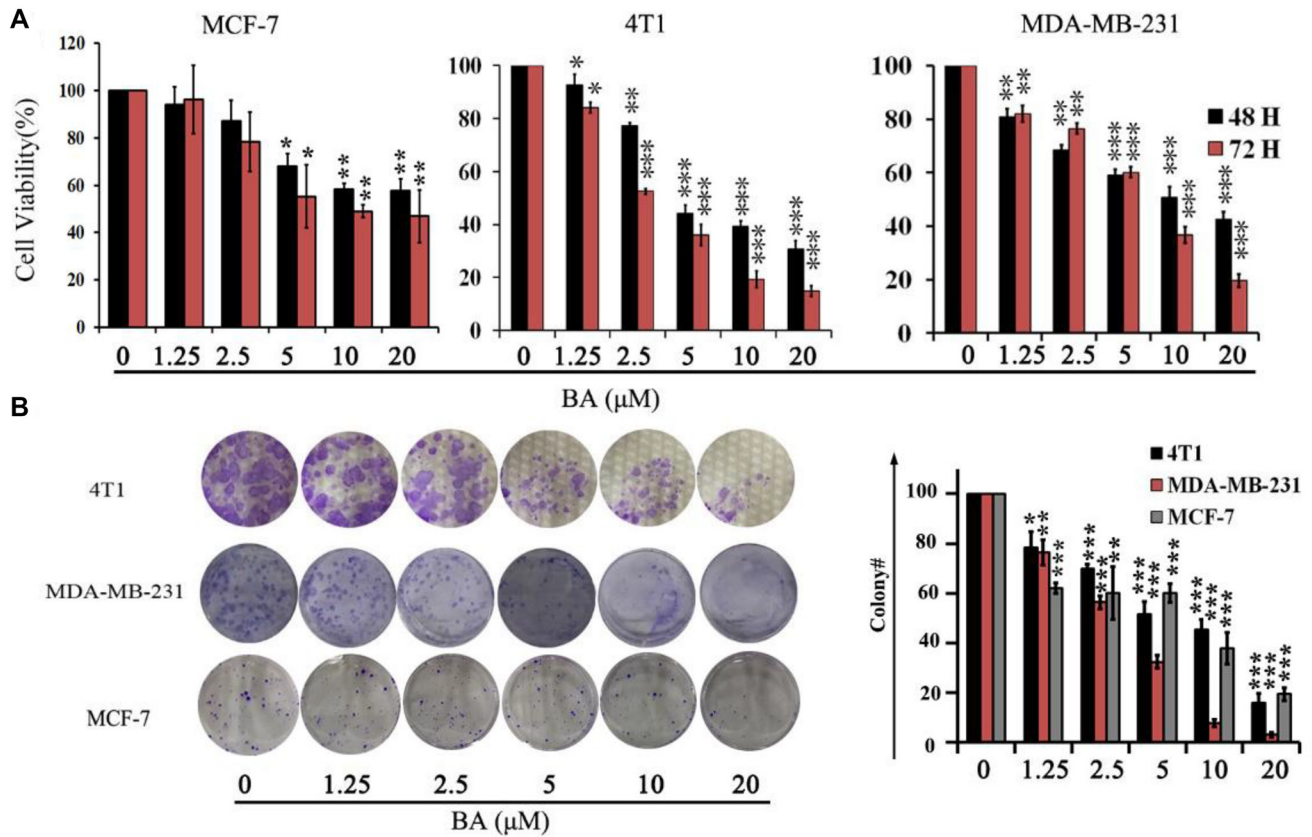


Figure 1: The effects of BA in breast cancer cells viability. (A) Proliferation of MCF-7, 4T1 and MDA-MB-231 cells treated with various concentrations (0–20 μM) of BA for 48 h and 72 h. Cell viability was evaluated by MTT assay. Data represent mean ± SD at least from 3 independent experiments. (B) The effects of BA (0–20 μM) on colony formation in 4T1, MDA-MB-231 and MCF-7 cell lines for 12 days, the statistic results of colony formation assays presented surviving colonies. Data are expressed as mean ± SD at least from 3 independent experiments ($P < 0.05$; $**P < 0.01$; $***P < 0.001$).

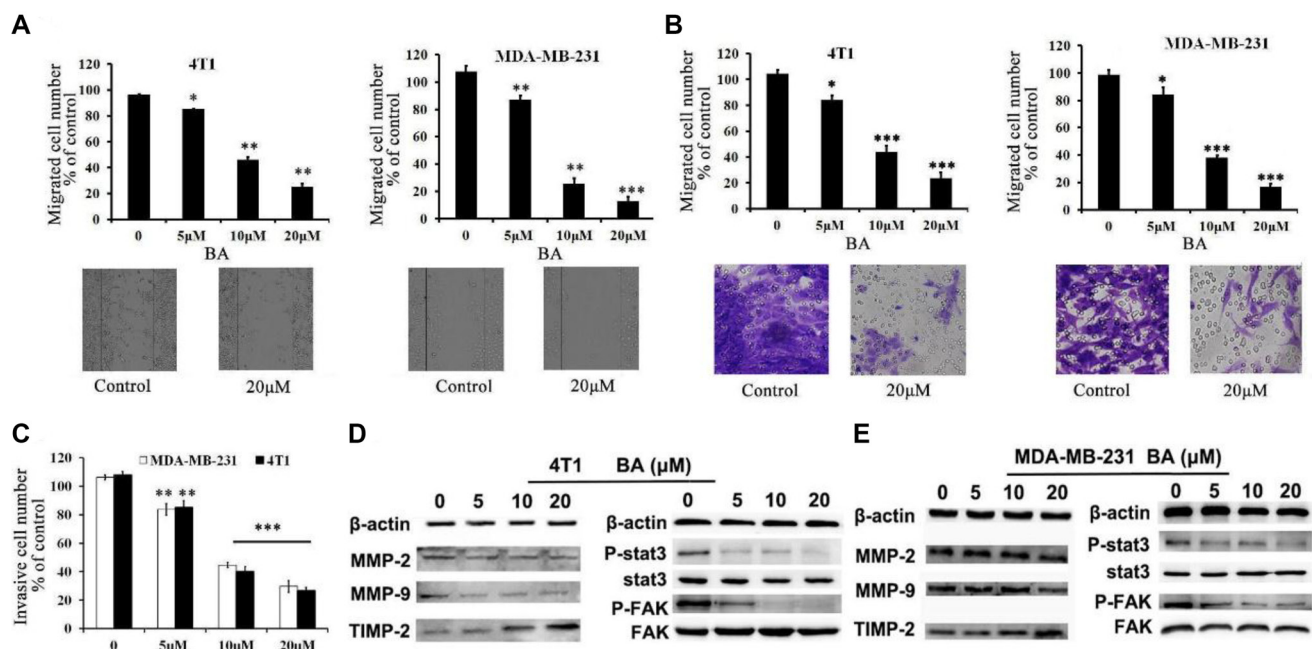


Figure 2: BA inhibits breast cancer cells 4T1 and MDA-MB-231 migration and invasion. (A) Tumor cells were seeded in six-well plates. We make a 'wound' after the cells grew ~90% confluence. After incubation for 48 h, the groups were graphed. The black lines indicate the section occupied by the initial scraping, and migrated cells were quantified. (B) Tumor cells were seeded in the roof chamber of transwell with serum-free medium and treated with vehicle or different concentrations of BA. After 48 h, migrated cells were fixed, stained and graphed (20×) and quantified. (C) BA inhibits 4T1 and MDA-MB-231 invasion. Tumor cells were treated with different concentrations of BA and invaded through Matrigel. Invaded cell number was counted ($P < 0.05$; $**P < 0.01$; $***P < 0.001$). (D, E) 4T1 and MDA-MB-231 cells were treated with different concentrations of BA. After 48 h, cells were harvested, and western blot assay was performed to detect the expression of MMP-2, MMP-9, TIMP-2, Stat3, P-Stat3, FAK, P-FAK. β -actin served as loading control.

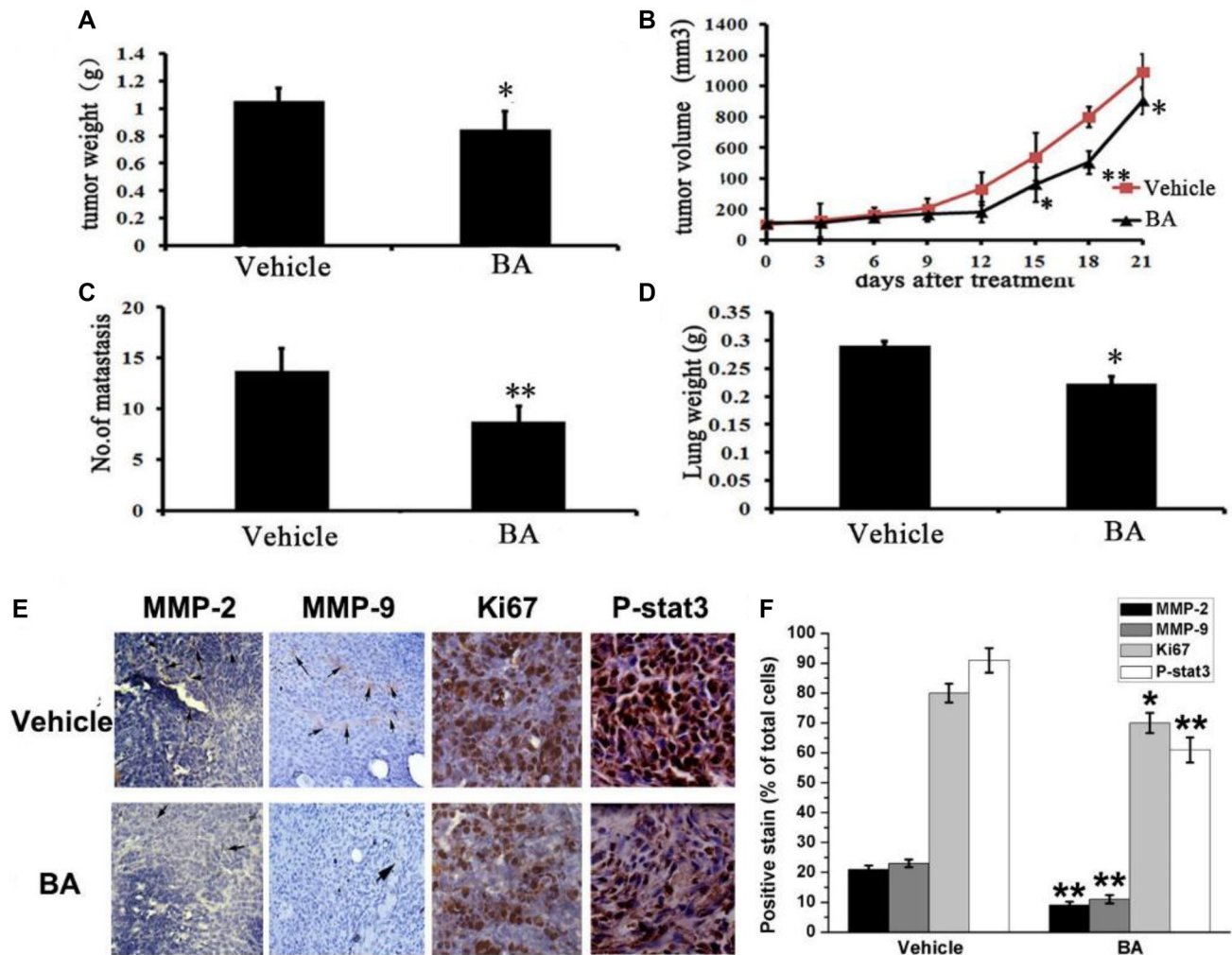


Figure 3: Anti-tumor and anti-metastasis effects of BA *in vivo*. (A) Represented weight of tumor from mice of different groups (vehicle and BA (10 mg/kg/day)), respectively. Data were mean \pm SD ($n = 6$; $*P < 0.05$). (B) Tumor volume were measured and calculated every three days and presented as mean \pm SD ($n = 6$; $*P < 0.05$, $**P < 0.01$). (C) The number of metastasis from lungs. Data were mean \pm SD ($n = 6$; $*P < 0.05$). (D) The lungs weight of different groups. Results were mean \pm SD ($n = 6$; $**P < 0.01$). (E) Immunohistochemistry was performed to measure the expression of MMP-2, MMP-9, Ki67 and P-Stat3 in tumor tissues isolated from vehicle and BA-treated (10 mg/kg/day) mice. (F) The treatment with BA markedly reduced MMP-2, MMP-9, Ki67 and P-Stat3-positive cells versus vehicle group (20 \times).

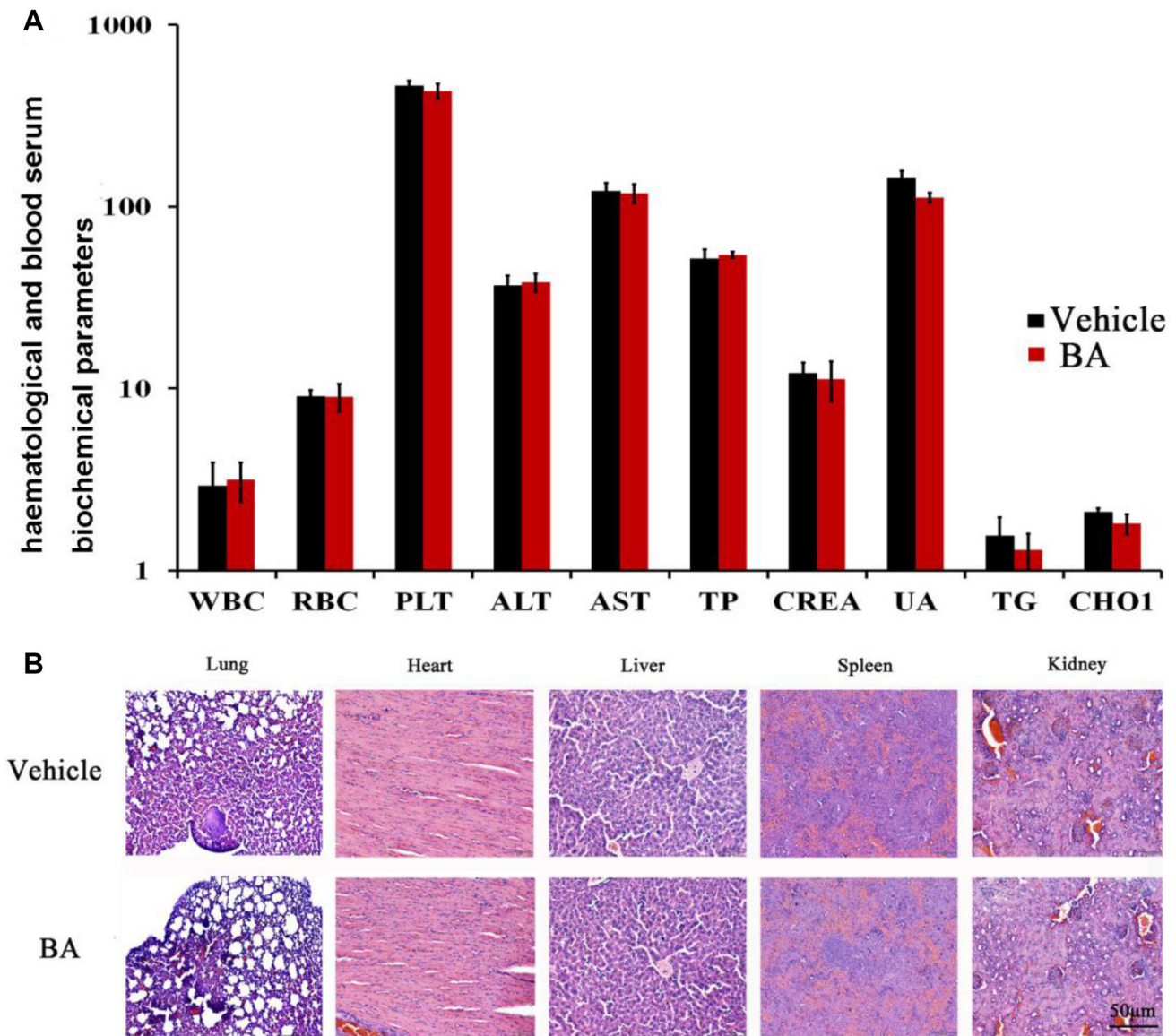


Figure 5: Evaluation of side effects of BA in mice. (A) Hematological and serum biochemistry analysis of blood were done. Units of the parameters are as follows. WBC (white blood cell) and PLT (platelet), $10^9/l$; RBC (red blood cell), $10^{12}/l$; TP (total protein), g/l; ALT (alanine transaminase) and AST (aspartate aminotransferase), U/l; CREA (creatinine) and UA (uric acid), μM ; TG (triglyceride) and CHOL (cholesterol), mM. (B) BA did not cause obvious pathologic abnormalities in normal tissues. H&E staining of paraffin-embedded sections of the lung, heart, liver, spleen and kidney (20 \times).